NUMERICAL EVALUATION OF GROUNDWATER-LEVEL EFFECTS ON THE SEISMIC RESPONSE OF A MULTISTORY BUILDING–SOIL SYSTEM USING PLAXIS 3D

Yuldashev Sharafitdin[1], **Boytemirov Muxamadbobir**[2], **Abdunazarov Akbarjon**[3], **Yuldashev Faxriddin**[4], **Vahobov Boburkhon**[5]
Doctor of Technical Sciences, Professor[1]
PhD in Technical Sciences, Associate Professor[2]
PhD Student[3]
PhD in Technical Sciences[4]
PhD in Technical Sciences[5]

DOI: 10.67620/sai.58a0010

ABSTRACT
Groundwater conditions can alter the effective stress state and mass characteristics of foundation soils and thereby influence seismic soil–structure interaction. This study evaluated the effect of groundwater level (GWL) on the seismic response of a multistory building–soil system using three-dimensional finite-element modeling in PLAXIS 3D. The computational domain comprised three soil layers extending from the ground surface to a depth of 50 m and represented by the Mohr–Coulomb constitutive model under drained conditions. Two controlled models were analyzed with GWLs of −50 m and −3 m. Geometry, material properties, the building model, finite-element mesh, monitoring locations, and the same 0–10 s real earthquake accelerogram were held constant so that groundwater level was the only intentionally varied condition. Horizontal displacement, velocity, and acceleration time histories were compared at a soil monitoring node and at the first and ninth floors. The maximum downward vertical displacement was −48.37 mm and was concentrated within the foundation influence zone. At the soil node, several velocity and acceleration peaks were larger for GWL = −3 m, whereas horizontal displacement histories were nearly coincident. First-floor responses were similar between cases, while ninth-floor acceleration exceeded first-floor acceleration. The findings indicate that groundwater level should be treated as an independent variable in seismic soil–structure interaction analyses and that acceleration and velocity may be more sensitive to groundwater changes than displacement under the modeled conditions.

ACCEPTED

07.09.26

Keywords: *groundwater level, seismic response, soil–structure interaction, PLAXIS 3D, finite-element analysis.*

CC BY

Introduction

Numerical Evaluation of Groundwater-Level Effects on the Seismic Response of a Multistory Building–Soil System Using PLAXIS 3D

The seismic performance of buildings in earthquake-prone regions depends not only on the characteristics of the structural system but also on the physical, mechanical, and hydrogeological conditions of the foundation soil (Abdunazarov et al., 2026; Ismailov et al., 2025; Savutov et al., 2026; Yuldashev et al., 2025). During an earthquake, ground motion propagates through the soil to the foundation and subsequently into the superstructure (Il'ichev et al., 1999; Ismoilov et al., 2025; Yuldashev et al., 2026). Soil density, stiffness, stratification, porosity, and groundwater level can therefore influence both the amplitude and the temporal characteristics of the seismic signal reaching the structure (Abdunazarov & Soliev, 2020; Mirsaidov et al., 2021; Yuldashev et al., 2023).

Natural soil is a multiphase medium consisting of a solid mineral skeleton, pore water, and air. When groundwater is deep, much of the soil domain remains unsaturated. As the water table rises, the degree of saturation, bulk mass density, and effective stress state change. Because water is substantially less compressible than air, increasing saturation can alter the bulk response of the soil, while pore-water pressure affects the effective stress carried by the soil skeleton (Abdunazarov, 2022a; Abdunazarov, 2023; Kholmirzayev et al., 2022; Yuldashev & Abdunazarov, 2023). Consequently, groundwater-level changes need not influence displacement, velocity, and acceleration in the same manner (Yuldashev et al., 2022).

A controlled numerical comparison is necessary to isolate the groundwater-level effect. The geometry, constitutive parameters, structural model, finite-element mesh, and seismic input should remain unchanged between the cases being compared (Abdunazarov, 2022c; Yuldashev & Abdunazarov, 2024a). When these quantities are held constant, differences in the computed response can be associated more directly with the hydrogeological condition (Abdunazarov, 2022b; Yuldashev & Abdunazarov, 2024c). This approach is particularly important for a real earthquake accelerogram because the response evolves over time, and a single maximum displacement value cannot fully describe the dynamic behavior of a soil–structure system (Yuldashev & Abdunazarov, 2024b, 2024d).

Accordingly, the objective of this study was to compare two three-dimensional PLAXIS models of the same multistory building–soil system with groundwater levels of −50 m and −3 m under an identical real earthquake accelerogram. The analysis focused on how the hydrogeological condition affected horizontal displacement, velocity, and acceleration at a soil monitoring node and at different elevations of the building (Yuldashev & Abdunazarov, 2024e).

Method

Seismic-Wave Parameters and Dynamic Soil Properties

For an equivalent single-phase elastic medium, the velocities of compressional (P) and shear (S) waves depend on bulk stiffness, shear stiffness, and mass density. The relationships used to describe these dependencies are

$$V_p = \sqrt{[(K + 4G/3)/\rho]} \quad (1)$$

$$V_s = \sqrt{(G/\rho)} \quad (2)$$

where K is the bulk modulus, G is the shear modulus, and ρ is mass density. Rayleigh-wave velocity is generally close to S-wave velocity and may be estimated as $V_r \approx (0.87–0.95)V_s$. Because groundwater-level variations alter density, effective stress, and the stiffness state of the soil skeleton, the conditions governing seismic-wave transmission may also change (Ismailov et al., 2025; Savutov et al., 2026; Yuldashev et al., 2025).

Wavelength (λ) is related to wave velocity (V) and frequency (f) by

$$\lambda = V/f \quad (3)$$

A real earthquake accelerogram contains multiple frequency components. Consequently, changes in dynamic soil properties and wave velocity can modify the time-dependent response. No separate frequency-domain or modal analysis was performed in this study; the results were therefore interpreted directly from computed time histories and their approximate extreme values.

ISSN: 2181-3337 | SCIENTISTS.UZ

Groundwater Level and Effective Stress

For soil below the groundwater table, the relationship between total and effective stress follows Terzaghi's effective stress principle:

$$\sigma' = \sigma - u \quad (4)$$

where σ′ is effective stress, σ is total stress, and u is pore-water pressure. Raising the groundwater level changes the initial hydrostatic condition and the unit weight of the soil below the water table. These changes can modify both the deformation field beneath the foundation and the transmission of dynamic motion. In the present study, the effects were evaluated from displacement, velocity, and acceleration time histories.

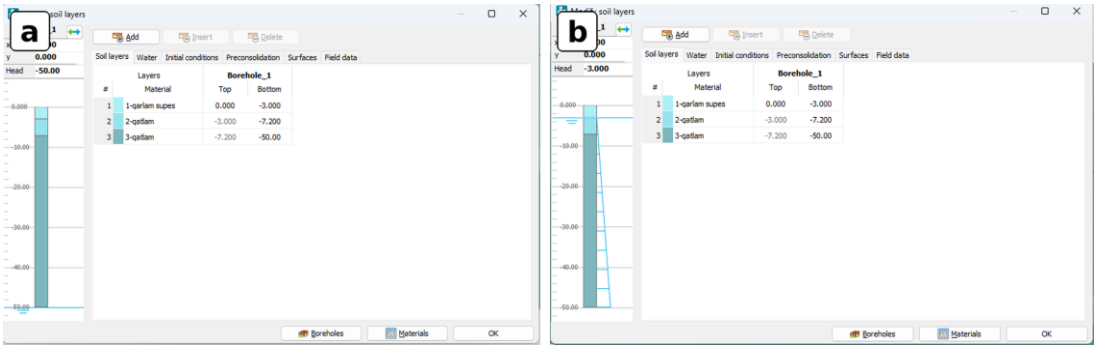
Numerical Model and Analysis Procedure

Soil Profile and Groundwater Scenarios

The computational domain comprised a three-layer soil mass extending to a depth of 50 m. Layer 1 occupied the interval from 0 to −3.0 m, Layer 2 from −3.0 to −7.2 m, and Layer 3 from −7.2 to −50.0 m. Two hydrogeological cases were modeled. In Case 1, the groundwater level was placed at −50 m; in Case 2, it was placed at −3 m. Thus, in Case 2, the soil below −3 m was below the water table, while all other geometric and mechanical conditions were unchanged. Figure 1 illustrates the two groundwater-level scenarios.

Figure 1

Groundwater-Level Scenarios for the Layered Soil Profile



Note. (a) GWL = −50 m; (b) GWL = −3 m. GWL = groundwater level.

The basic physical and mechanical properties of the soil layers are summarized in Table 1, and the porosity and wave-velocity parameters are provided in Table 2.

Table 1

Basic Physical and Mechanical Properties of the Soil Layers

Layer	Depth (m)	γunsat (kN/m³)	γsat (kN/m³)	Eref (MPa)	ν	c′ (kPa)	φ′ (°)
Layer 1	0 to −3.0	17	18	12	0.35	1	31
Layer 2	−3.0 to −7.2	18	19	30	0.30	24	18
Layer 3	−7.2 to −50.0	19	20	90	0.30	0	33

Note. All soil layers were modeled using the Mohr–Coulomb model under drained conditions, with a dilatancy angle ψ = 0°. γunsat = unsaturated unit weight; γsat = saturated unit weight; Eref = reference Young's modulus; ν = Poisson's ratio; c′ = effective cohesion; φ′ = effective friction angle.

Table 2

Porosity and Wave-Velocity Parameters

Layer	einit	ninit	Vs (m/s)	Vp (m/s)	Constitutive model
Layer 1	0.5000	0.3333	50.64	105.4	Mohr–Coulomb
Layer 2	0.5000	0.3333	79.30	148.4	Mohr–Coulomb
Layer 3	0.5000	0.3333	133.7	250.1	Mohr–Coulomb

Note. einit = initial void ratio; ninit = initial porosity; Vs = shear-wave velocity; Vp = compressional-wave velocity.

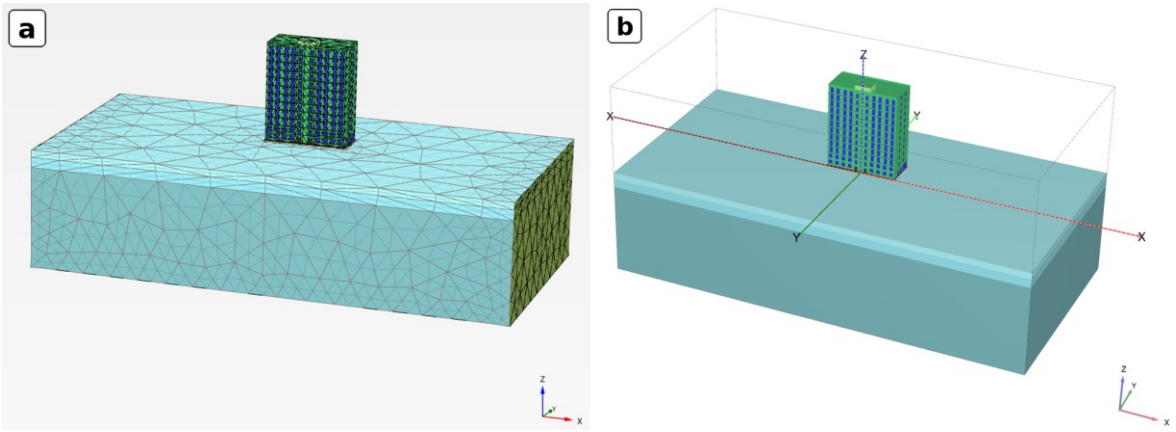
ISSN: 2181-3337 | SCIENTISTS.UZ

Building–Soil System and Finite-Element Mesh

The multistory building and the soil mass were modeled as a unified three-dimensional finite-element system. For both hydrogeological cases, building geometry, soil stratification, material parameters, finite-element mesh, and the overall computational scheme were kept identical. All technical settings of the dynamic analysis were likewise held constant. This controlled design allows differences in response to be attributed primarily to groundwater-level variation. Figure 2 shows the model mesh and overall geometry.

Figure 2

Three-Dimensional Numerical Model of the Multistory Building–Soil System



Note. (a) Finite-element mesh; (b) overall geometry of the soil layers and building.

Seismic Input, Analysis Cases, and Monitoring Points

The same real earthquake accelerogram, covering the interval from 0 to 10 s, was applied to both models. Monitoring nodes were selected in the soil, at the first floor, and at the ninth floor of the building. At these locations, time histories of horizontal displacement (u_x), velocity (v_x), and acceleration (a_x) were obtained. The comparison considered extreme values, the temporal form of the response curves, the locations of prominent peaks, and the variation of response with building height. Table 3 summarizes the two analysis cases.

Table 3

Comparison of the Numerical Analysis Cases

Parameter	Case 1: Deep GWL	Case 2: Shallow GWL
Groundwater level	−50 m	−3 m
Unit weight	γunsat	γsat below groundwater level
Soil model	Mohr–Coulomb, drained	Mohr–Coulomb, drained
Geometry and mesh	Identical	Identical
Seismic input	Same real accelerogram, 0–10 s	Same real accelerogram, 0–10 s
Monitoring	Soil node; 1st and 9th floors	Soil node; 1st and 9th floors

Note. GWL = groundwater level. The geometry, mechanical properties, mesh, monitoring points, and seismic input were identical between cases.

Results and Discussion

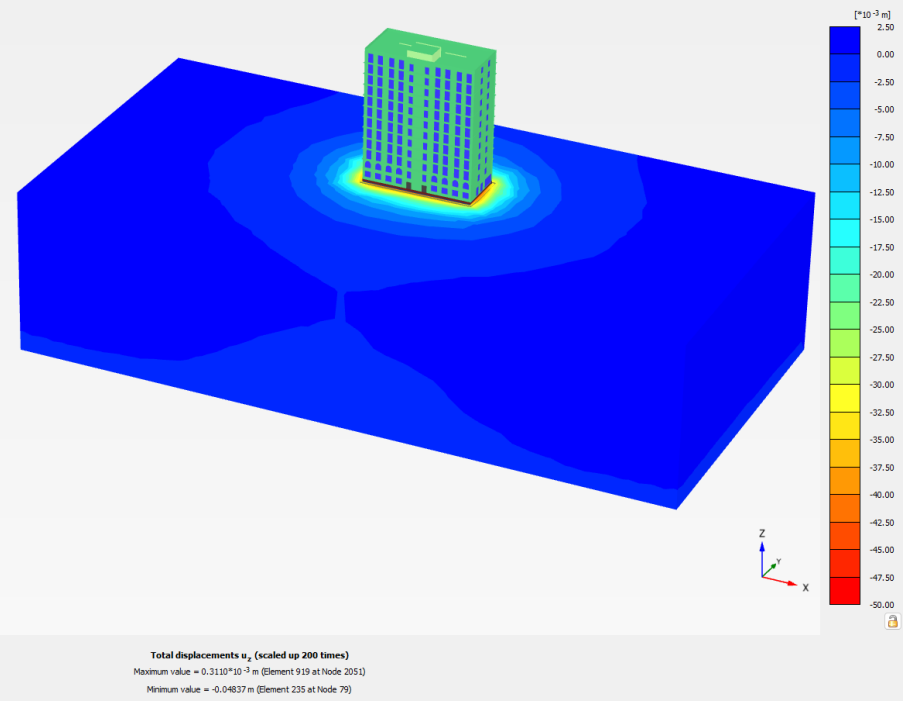
Vertical Displacement Field

The numerical results showed that the largest vertical displacements were concentrated around the building foundation. The contour field decreased outward from the area beneath the foundation. The maximum upward displacement was 0.311 mm, whereas the maximum downward displacement reached −48.37 mm. This distribution indicates that vertical deformation was concentrated within the soil–structure interaction zone adjacent to the foundation (Figure 3).

ISSN: 2181-3337 | SCIENTISTS.UZ

Figure 3

Vertical Displacement Field of the Building–Soil System



Response at the Soil Monitoring Node

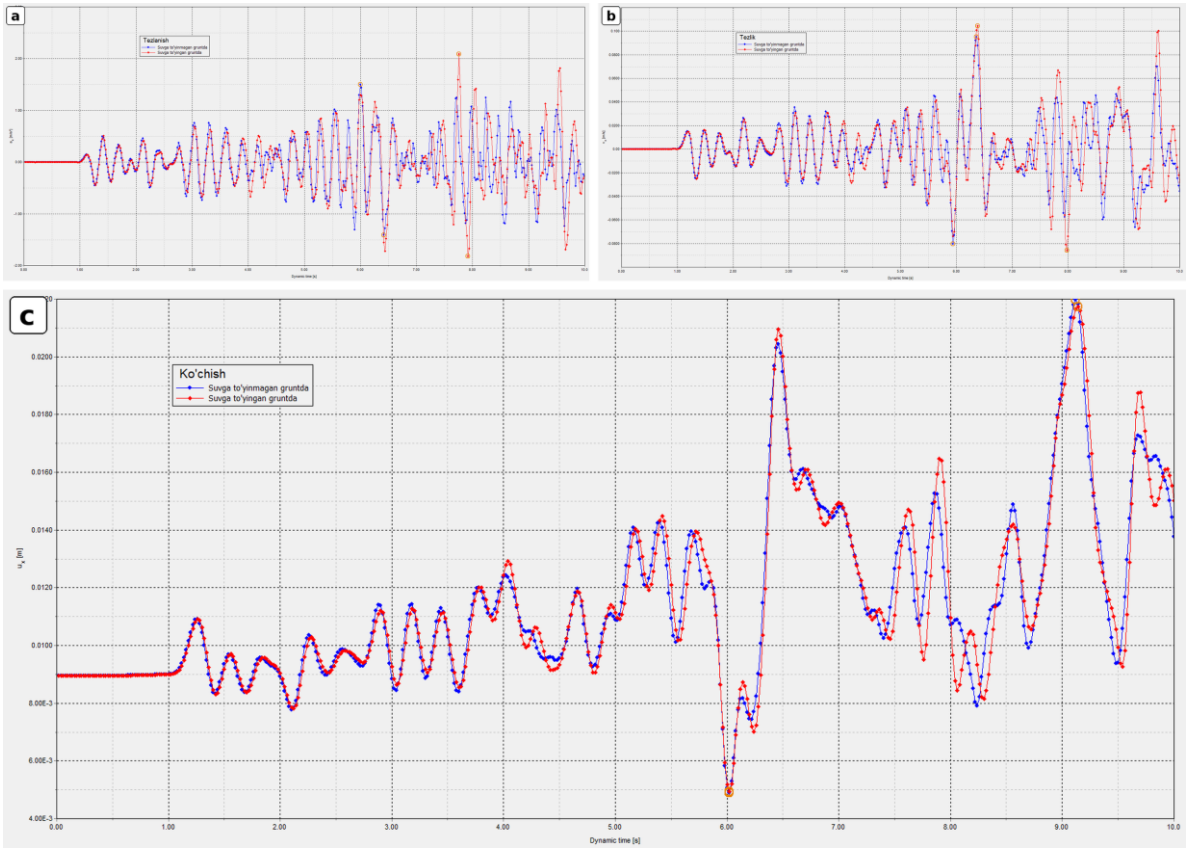
Acceleration, velocity, and horizontal-displacement time histories at the soil monitoring node were compared for the two hydrogeological cases (Figure 4). The response curves were close during the initial portion of the record, whereas differences between several peaks became more pronounced during later strong pulses. Based on the graph scale, the GWL = −3 m case reached an approximately +2.1 m/s² positive acceleration peak and a −1.8 m/s² negative peak; the corresponding extrema for GWL = −50 m were approximately +1.5 and −1.4 m/s². Thus, for several portions of the selected seismic record, the shallower groundwater condition was associated with a larger acceleration response at the soil monitoring node.

In the velocity history, the GWL = −3 m case reached approximately +0.105 m/s and −0.086 m/s, slightly exceeding the corresponding values for the GWL = −50 m case. By contrast, the horizontal-displacement histories were nearly coincident, with a maximum value close to 0.022 m. Under the conditions of the present model and accelerogram, groundwater-level variation was therefore more evident in velocity and especially in acceleration than in displacement.

ISSN: 2181-3337 | SCIENTISTS.UZ

Figure 4

Time Histories at the Soil Monitoring Node



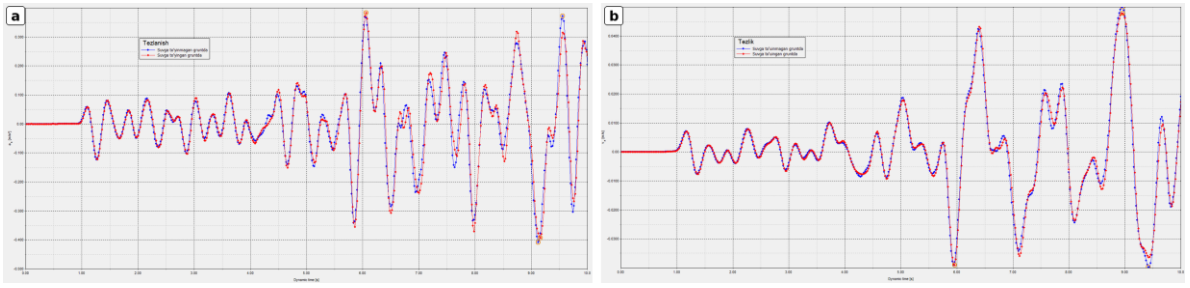
Note. (a) Acceleration a_x; (b) velocity v_x; (c) horizontal displacement u_x. In the source plots, blue represents GWL = −50 m and red represents GWL = −3 m.

First-Floor Response

At the first-floor monitoring node, acceleration and velocity time histories had similar forms for the two groundwater-level cases (Figure 5). From the plot scale, acceleration varied approximately from −0.41 to +0.38 m/s² and velocity from −0.040 to +0.049 m/s. Although small differences appeared at several local peaks, the overall amplitude ranges and temporal responses remained close. Under the selected computational conditions, the influence of groundwater-level variation on the first-floor kinematic response was therefore more limited than at the soil monitoring node.

Figure 5

Time Histories at the First Floor of the Building



Note. (a) Acceleration; (b) velocity.

Ninth-Floor Acceleration Response

Acceleration amplitude at the ninth floor was greater than at the first floor, reaching approximately −0.63 to +0.92 m/s² according to the graph scale. The overall forms of the time histories remained similar for the two groundwater-level cases, although individual peak amplitudes differed: GWL = −50 m produced the larger value at some positive maxima, whereas GWL = −3 m produced the larger absolute value at some negative maxima. This result indicates that seismic response was not distributed uniformly with building height and that dynamic amplification occurred at the upper floor. Because no separate modal

ISSN: 2181-3337 | SCIENTISTS.UZ

analysis was performed, the observed amplification was not assigned to a specific vibration mode (Figure 6).

Figure 6

Acceleration Time History at the Ninth Floor of the Building

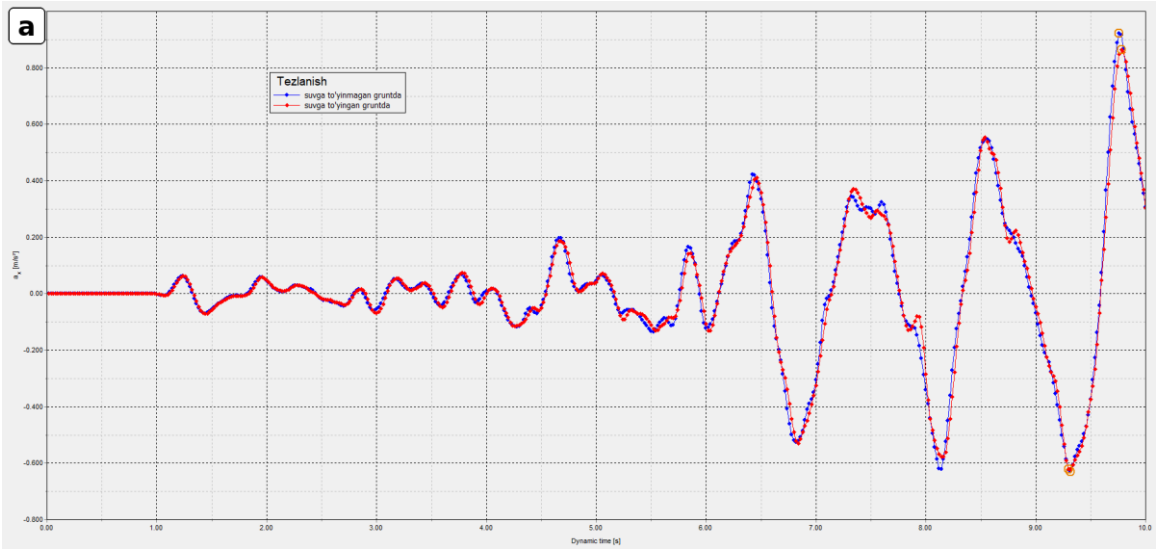


Table 4 summarizes the approximate extreme values read from the time-history plots. These values should be interpreted as plot-based estimates rather than direct numerical exports.

Table 4

Approximate Extreme Values Read From the Time-History Plots

Monitoring point	Parameter	GWL = −50 m	GWL = −3 m	Main observation
Soil	a_x (m/s²)	≈ −1.4 to +1.5	≈ −1.8 to +2.1	Several peaks are higher for GWL = −3 m
Soil	v_x (m/s)	≈ −0.080 to +0.095	≈ −0.086 to +0.105	Small but noticeable increase for GWL = −3 m
Soil	u_x (m)	≈ 0.0048 to 0.0220	≈ 0.0049 to 0.0219	Curves are nearly coincident
1st floor	a_x (m/s²)	≈ −0.41 to +0.38	≈ −0.39 to +0.38	Amplitudes are similar
1st floor	v_x (m/s)	≈ −0.040 to +0.049	≈ −0.039 to +0.048	Difference is very small
9th floor	a_x (m/s²)	≈ −0.61 to +0.92	≈ −0.63 to +0.87	Amplitude exceeds that at the 1st floor

Note. Values are approximate because several extrema were read from the graph scales rather than exported directly from PLAXIS Output. GWL = groundwater level.

Interpretation of Groundwater-Level Effects

The findings show that the groundwater-level effect depends on both the kinematic parameter and the location of observation. At the soil node, GWL = −3 m produced larger acceleration and velocity peaks, while horizontal displacement remained almost unchanged. Differences between the two cases were small at the first floor, whereas acceleration amplitude at the ninth floor was larger than at the first floor. Evaluating the groundwater effect from a single maximum displacement value would therefore provide an incomplete description of the system's dynamic behavior.

Because the same real accelerogram was imposed in both hydrogeological cases, the observed response differences can be associated with the changed initial hydrogeological condition and the resulting equivalent dynamic response of the soil. At the same time, the broadly similar forms of most time histories indicate that the principal temporal structure of the input motion was transmitted through both models. No fast Fourier transform, response-spectrum, or modal analysis was conducted; therefore, the observed amplitude differences cannot be assigned to a specific frequency band or structural vibration mode.

Limitations and Reliability Considerations

The soil layers were represented by the Mohr–Coulomb model under drained conditions. This formulation is appropriate for a controlled comparison of the two hydrogeological cases, but it does not fully represent the nonlinear dependence of soil stiffness on strain level and effective stress. For a more detailed investigation of small-strain dynamic behavior, an advanced constitutive formulation such as HSsmall can account explicitly for small-strain stiffness parameters such as G_0^{ref} and $\gamma_{0.7}$ (Yuldashev et al., 2023, 2026).

The present Mohr–Coulomb, drained results should not be interpreted as a complete representation of cyclic excess pore-water-pressure accumulation or liquefaction in saturated soil. In addition, because several extreme values reported in this paper were read from plot scales, the quantitative conclusions should be verified using direct numerical exports from PLAXIS Output (Abdunazarov, 2023; Yuldashev & Abdunazarov, 2023; Yuldashev et al., 2022). Sensitivity analyses with several mesh densities and time-step sizes would further strengthen confidence in numerical stability (Abdunazarov, 2022a).

Future work should investigate intermediate groundwater levels, multiple real earthquake accelerograms, direct comparisons between Mohr–Coulomb and HSsmall soil models, time-history responses of pore-water pressure and effective stress, and frequency-domain measures such as fast Fourier transforms and response spectra.

Conclusion

Two three-dimensional multistory building–soil models with groundwater levels of −50 m and −3 m were compared in PLAXIS 3D under the same real earthquake accelerogram while geometric, physical-mechanical, and computational conditions were kept identical. The results demonstrate that groundwater-level changes did not affect displacement, velocity, and acceleration to the same degree. The most pronounced differences occurred in velocity and acceleration at the soil monitoring node, where several extreme values were higher for GWL = −3 m. Horizontal-displacement histories, however, were almost coincident. Under the conditions of the selected model and input record, velocity and acceleration were therefore more sensitive to groundwater-level variation than displacement.

The maximum downward vertical displacement was −48.37 mm, and the principal deformation was concentrated in the soil–structure interaction zone near the foundation. Velocity and acceleration responses at the first floor were similar between hydrogeological cases, whereas ninth-floor acceleration amplitude exceeded that at the first floor. These findings indicate that the groundwater-level effect is not manifested uniformly throughout the soil and building and that seismic response can be amplified with building height.

The results do not support a general assumption that increased soil saturation will always reduce or always increase seismic vibration. The response of the building–soil system is governed jointly by soil stiffness, mass density, effective stress, groundwater level, the time-dependent characteristics of the accelerogram, and the dynamic behavior of the structure. Groundwater level should therefore be treated as an independent variable in seismic soil–structure interaction analyses. Future studies should evaluate several groundwater levels and multiple earthquake records and should assess displacement, velocity, and acceleration comprehensively in both the soil and the structure.

REFERENCES

1. Abdunazarov, A. (2022a). Analyses on improving measures to determine and reduce the impact of vibrations generated by vehicle movement on buildings. *Science and Innovation, 1*(A5), 372–375. https://doi.org/10.5281/zenodo.7066624
2. Abdunazarov, A. (2022b). Improving measures to determine and reduce the impact of vibrations on buildings. *Science and Innovation, 1*(A5), 380–384.
3. Abdunazarov, A. (2022c). Improving measures to determine and reduce the impact of vehicle-induced vibrations on buildings using local raw material (reed). *Science and Innovation, 1*(A5), 380–385.

ISSN: 2181-3337 | SCIENTISTS.UZ

4. Abdunazarov, A. S. (2023). Analysis of deformation and seismic-wave propagation in water-saturated loess soils along highways. *Construction and Education, 1*(3), 60–65.
5. Abdunazarov, A., & Soliev, N. (2020). Study of the performance of frameless construction structures under the influence of vertical stresses of ultra-submerged loess soils. *Student Bulletin*, (28-3), 39–40.
6. Abdunazarov, A., Yuldashev, S., Boytemirov, M., Karabayeva, M., & Yuldashev, F. (2026). Seismic surface-wave protection of the administrative building of Namangan State Technical University using a tire-filled barrier. *Vibroengineering Procedia, 62*, 668–674. https://doi.org/10.21595/vp.2026.26127
7. Il'ichev, V. A., Yuldashev, S. S., & Matkarimov, P. Z. (1999). Forced vibrations of an inhomogeneous planar system with passive vibrational insulation. *Soil Mechanics and Foundation Engineering, 36*(2), 50–54. https://doi.org/10.1007/BF02469084
8. Ismailov, V. A., Rakhmatov, A. R., Xusomiddinov, A. S., Yadigarov, E. M., & Bozorov, J. Sh. (2025). Assessment of the soil seismic condition through microseismic measurements: A case study of Bukhara. *News of the National Academy of Sciences of the Republic of Kazakhstan, Series of Geology and Technical Sciences, 5*(473), 131–145. https://doi.org/10.32014/2025.2518-170X.554
9. Ismoilov, V. A., Khusomiddinov, A. S., Mukhammadkulov, N. M., Yadigarov, E. M., Khayriddinov, B. B., Rakhmatov, A. R., Jumaev, D. D., Bozorov, J. Sh., Isroilov, X. B., & Mansurov, A. F. (2025). Assessment of landslide dynamics based on microseismic parameters. *Seismic Instruments, 61*, 346–353. https://doi.org/10.3103/S0747923925700446
10. Kholmirzayev, S., Akhmedov, I., Khamidov, A., Umarov, I., Axmedov, A., & Abdunazarov, A. (2022). Prospects for the development of reinforced concrete structures in Uzbekistan. *Science and Innovation, 1*(A8), 1052–1057.
11. Mirsaidov, M., Boytemirov, M., & Yuldashev, F. (2021). Estimation of the vibration waves level at different distances. In *Proceedings of FORM 2021: Construction—The Formation of Living Environment* (pp. 207–215). Springer. https://doi.org/10.1007/978-3-030-79983-0_19
12. Savutov, R., Shamuratov, A., Ismailov, V., Yodgorov, S., & Abdunazarov, A. (2026). Assessing the seismic vulnerability of single-family residential buildings in the Khorezm region. *Vibroengineering Procedia, 62*, 189–194. https://doi.org/10.21595/vp.2026.26187
13. Yuldashev, S. S., & Abdunazarov, A. S. (2023). Identification of seismic surface waves affecting a building and their reduction using a seismic barrier (polyurethane foam). In *Science and Innovation–2023: Development and Priority Directions: Republican Scientific-Practical Conference* (pp. 198–201).
14. Yuldashev, S. S., & Abdunazarov, A. S. (2024a). Advantages of circular and rectangular seismic barriers. *Journal of Transport, 1*(3), 91–93.
15. Yuldashev, S. S., & Abdunazarov, A. S. (2024b). Determining the effectiveness of seismic barriers by changing their height. *Science and Innovation, 3*(A8), 48–56. https://doi.org/10.5281/zenodo.13623022
16. Yuldashev, S. S., & Abdunazarov, A. S. (2024c). Determining the effectiveness of seismic barriers by changing their thickness. *Science and Innovation, 3*(A8), 27–34. https://doi.org/10.5281/zenodo.13350631
17. Yuldashev, S. S., & Abdunazarov, A. S. (2024d). Determining the effectiveness of distance placement of a seismic barrier in protecting buildings from seismic waves. *Journal of Transport, 1*(3), 124–126.
18. Yuldashev, S. S., & Abdunazarov, A. S. (2024e). Determining the efficiency of seismic barriers based on their horizontal and vertical positioning. *Science and Innovation, 3*(A8), 40–47. https://doi.org/10.5281/zenodo.13386720
19. Yuldashev, S. S., Boytemirov, M. B., Yuldashev, F. S., & Abdunazarov, A. S. (2022). Effect of vehicle-traffic-induced vibration on buildings. *Mechanics and Technology, 4*(9), 19–29.

20. Yuldashev, S. S., Alimov, X. L., Abdunazarov, A. S., Yuldasheva, G., & Xakimov, X. A. (2023). Effect of groundwater level on the propagation of seismic surface waves. In *Innovations in Construction and Seismic Safety of Buildings and Structures: International Scientific and Technical Conference* (pp. 314–318).
21. Yuldashev, S., Abdunazarov, A., Jumaboyeva, S., Boytemirov, M., & Tillaboyev, Y. (2025). Attenuation of seismic surface waves affecting the building using various barriers. *AIP Conference Proceedings, 3265*, 030016. https://doi.org/10.1063/5.0265304
22. Yuldashev, S. S., Boytemirov, M. B., & Abdunazarov, A. S. (2026). Evaluation of the effectiveness of strengthening the foundation soil of multistory buildings using a soil cushion and deep soil mixing technology in reducing seismic effects. *Science and Innovation, 5*(6), 33–42. https://doi.org/10.5281/zenodo.20697242

ISSN: 2181-3337 | SCIENTISTS.UZ